

**Stabilization, rolling and addition of other ECM proteins to collagen hydrogels improves regeneration in chitosan guides for long peripheral nerve gaps in rats.**

Francisco Gonzalez-Perez<sup>1</sup> PhD, Stefano Cobiachi<sup>1</sup> PhD, Claudia Heimann<sup>2</sup> PhD, James B Phillips<sup>3</sup> PhD, Esther Udina<sup>1</sup> MD, PhD, Xavier Navarro<sup>1</sup> MD, PhD.

<sup>1</sup>Institute of Neurosciences and Department of Cell Biology, Physiology and Immunology, Universitat Autònoma de Barcelona, and CIBERNED, Spain.

<sup>2</sup>Medovent GmbH, Mainz, Germany.

<sup>3</sup>Biomaterials & Tissue Engineering, UCL Eastman Dental Institute, University College London, UK.

**\* Corresponding author:**

X. Navarro, Tel: +34-935811966; Fax: +34-935812986; Email: [Xavier.navarro@uab.cat](mailto:Xavier.navarro@uab.cat)

**Acknowledgements - Disclosures**

The authors report no disclosures and conflicts of interest. This study was supported by the European Community's Seventh Framework Programme (FP7-HEALTH-2011) under grant agreement n° 278612 (BIOHYBRID). Medical grade chitosan for manufacturing the chitosan tubes was supplied by Altakitin SA (Lisbon, Portugal). The authors thank Marta Morell and Jessica Jaramillo for their technical support.

**Abstract**

**BACKGROUND:** Autograft is still the gold standard technique for the repair of long peripheral nerve injuries. The addition of biologically active scaffolds into the lumen of a conduits to mimic the endoneurium of peripheral nerves may increase the final outcome of artificial nerve devices. Furthermore, the control of the orientation of the collagen fibers may provide some longitudinal guidance architecture providing a higher level of meso-scale tissue structure.

**OBJECTIVE:** The aim of this study is to evaluate the regenerative capabilities of chitosan conduits enriched with ECM-based scaffolds to bridge a critical gap of 15 mm in the rat sciatic nerve.

**METHODS:** The right sciatic nerve of female Wistar Hannover rats was repaired with chitosan tubes functionalized with ECM-based scaffolds fully hydrated or stabilized and rolled to bridge a 15 mm nerve gap. Recovery was evaluated by means of electrophysiology and algometry tests and histological analysis 4 months after injury.

**RESULTS:** Stabilized constructs enhanced the success of regeneration compared to fully hydrated scaffolds. Moreover, fibronectin-enriched scaffolds increased muscle reinnervation and number of myelinated fibers compared to laminin-enriched constructs.

**CONCLUSION:** A mixed combination of collagen and fibronectin may be a promising internal filler for neural conduits for the repair of peripheral nerve injuries, and their stabilization may increase the quality of regeneration over long gaps.

*Keywords:* chitosan, extracellular matrix, fibronectin, laminin, peripheral nerve, regeneration.

**Running head:** ECM in peripheral nerve regeneration

## Introduction

The use of artificial nerve conduits has emerged as an alternative to the classical autologous graft repair to bridge gaps in continuity of peripheral nerves after severe injuries<sup>1,2,3</sup>. Nerve conduits avoid some of the main problems associated with autograft repair, such as the additional surgical intervention to obtain the graft material, the mismatch between the injured nerve and the graft, and the limited source of donor nerves. Regeneration of peripheral nerves through artificial nerve guides is highly limited by the length of the gap, being poor for gaps longer than a critical length. Such critical gap length is dependent on the size of the nerve and the species<sup>4</sup>. Thus, when using standard silicone or plastic tubes, nerve regeneration occurs in the rat sciatic nerve if the gap is 10 mm or less but fails in most cases with 15 mm gaps<sup>5,6</sup>, whereas in the mouse sciatic nerve regeneration occurs in all cases with a 4 mm gap but fails with gaps 6 mm or longer<sup>7,8,9</sup>.

Current advances in the use of artificial nerve conduits to repair severe peripheral nerve lesions aim to create an internal milieu that mimics the natural microstructure found in a normal nerve<sup>1</sup>. An explored direction is the addition of biologically active scaffolds to the inner lumen that mimics the endoneurium of peripheral nerve tissue. The extracellular matrix (ECM) plays an important role in the proliferation and migration of Schwann cells, that guide the regenerating axons and their myelination<sup>10,11</sup> after nerve damage. Among other ECM components, laminin and fibronectin have a fundamental role in guiding the re-growth of damaged axons. Laminin and fibronectin have been both implicated in the regeneration of peripheral neurons *in vitro*<sup>12,13</sup> and *in vivo*<sup>14,15,16,17,18</sup>.

However, the incorporation of ECM-based scaffolds into nerve conduits has to take into account the matrix composition, density and the orientation of the fibrils, all factors that may influence the final outcome of the regeneration<sup>16,19</sup>. Cell and ECM alignment is a common feature of biological tissues, with anisotropy being critical to function in many instances<sup>20</sup>. The control of the orientation and direction of collagen fibers has been demonstrated to increase the invasion of neurites and Schwann cells from dorsal root ganglia cultured on the gel surface compared to unaligned collagen gels *in vitro*<sup>21</sup>. The range of approaches to achieve anisotropic engineered tissues include the use of aligned fibers, patterned surfaces, electrical and magnetic fields, mechanical gradient loadings or physical and chemical cues. Aligned cellular collagen-based hydrogels have been recently used to bridge peripheral nerve defects<sup>20</sup> reporting regeneration of peripheral nerves in a critical gap model of 15 mm in rats. In the experiments described here, we have compared the capability to support regeneration across a

non permissive 15 mm long defect of the sciatic nerve in the adult rat of chitosan conduits pre-filled with collagen I based matrices enriched with either laminin or fibronectin, and delivered as simple fully-hydrated hydrogels or stabilized by plastic compression and rolled to provide some longitudinal guidance architecture. Regardless of the cell and fibril level architecture, the meso-level anisotropy of the substrate may improve regeneration, since the matrix will serve to distribute the collagen fibers in a 3D space, and the anisotropic fibers will provide a 2D surface for regenerating axons<sup>22</sup>. By means of functional and morphological methods we assessed the effects of stabilized and rolled collagen-based matrices enriched with laminin or fibronectin to sustain nerve regeneration, migration of Schwann cells and axonal growth.

## Methods

### *Animals*

Adult female Wistar Hannover rats (Janvier), weighing 220-250 g, were housed in plastic cages under standard conditions *ad libitum*. All the experimental procedures were approved by the Ethical Committee of our institution and followed the rules of the European Communities Council Directive.

### *Preparation of conduits prefilled with extracellular matrix*

A solution of 800  $\mu$ l of rat tail type I collagen (BD-Biosciences) at a concentration of 3-4 mg/ml was mixed with 50  $\mu$ l of 10x Eagle's medium (Gibco) and 2  $\mu$ l of 7.5% sodium bicarbonate. For enriched matrices, 200  $\mu$ l (20% final volume) of human fibronectin (BD Biosciences) at 1 mg/ml or laminin type I (Sigma) at 1mg/ml (concentration of the solution) were added separately to the collagen type I mixed solution. The collagen concentration was then corrected to 2 mg/ml with extra PBS.

The manufacturing and characteristics of chitosan tubes were reported in a previous study<sup>23</sup>. For the preparation of fully hydrated gels, the chitosan tubes were carefully filled with the matrix preparations and kept in the incubator at 37°C for at least 30 minutes to allow matrix gel formation prior to implantation.

For the preparation of stabilized rolled hydrogels, the same matrix solutions were used to fill rectangular ABS moulds following the method described previously for cellular gels<sup>24</sup>. One ml of the mixture was added to each mould and integrated with tethering mesh at opposite ends. Tethered gels were covered with PBS and the moulds kept in the incubator at 37°C for 24 hours, then gels were separated from the tethering mesh and rapidly stabilized using

drying-compression with an absorbant pad. The resulting sheets were rolled (approximately 15 mm length) and placed into a longitudinally opened chitosan tube, which was closed with glue prior to implantation (Fig 1).

#### *Experimental design and surgical procedure*

For the study of regeneration over a critical sciatic nerve gap (15 mm), 37 rats were used. The animals were randomly assigned to one of five experimental groups in which the chitosan conduits contained: collagen I matrix (n=7, COL), laminin-enriched matrix (n=7, LM), fibronectin enriched matrix (n=8, FN), laminin-stabilized matrix (n=7, LM-St) and fibronectin-stabilized matrix (n=8; FN-St).

All surgical procedures were performed by the same researcher under aseptic conditions. Rats were anesthetized by intraperitoneal injection of ketamine/xylazine (90/10 mg/kg). Right sciatic nerves were exposed and cut 6 mm nerve segment was resected at a distance of 6 mm distal from the exit of the gluteal nerve. Then, nerve stumps were sutured with two epineural 10-0 sutures to 18 mm length chitosan devices with an internal diameter of 2 mm and leaving a 15 mm gap. The muscle plane and the skin were sutured with resorbable silk sutures and metallic clips and the wound was disinfected. Animals were treated with amitriptyline to prevent autotomy<sup>25</sup>.

For the study of Schwann cell migration 20 female Wistar Hannover rats were randomly distributed in the same experimental conditions (n=4 per group). We used a short sciatic nerve gap of 6 mm repaired with chitosan tubes of 9 mm in length. The operations were performed as described above.

#### *Electrophysiological tests*

Functional reinnervation of target muscles was assessed for the long gap study monthly up to 120 days. Animals were anesthetized and placed in a warm plate. Percutaneous electrodes were used to stimulate the sciatic nerve at the sciatic notch and register the compound muscle action potentials (CMAPs) and latencies of the M waves of distal muscles (tibialis anterior, gastrocnemius and plantar muscles)<sup>23</sup>.

#### *Functional evaluation of sensory recovery*

The threshold for nociceptive responses to mechanical and thermal stimuli was evaluated on both hindpaws by means of algometry tests monthly up to 122 dpo. For both tests, nociceptive responses were evaluated in the lateral part of the paw, which is the territory of

the plantar surface innervated by the sural branch of the sciatic nerve. The contralateral paw was used as control to overcome possible variations between testing conditions. To discard confounding effects due to collateral reinnervation of the saphenous nerve<sup>26</sup>, this nerve was resected after 120 dpo tests and they were repeated at 122 dpo.

Mechanical algesimetry measurements obtained in grams were obtained by an electronic Von Frey algesimeter (Bioseb, Chaville, France) whereas thermal algesimetry values measured in seconds were studied using a plantar algesimeter (Ugo Basile, Comerio, Italy). For both, a cutoff point was settled at 40 g or 20 s respectively. All values are presented the mean of three repetitive measures and as the percentage of response between the injured and non-injured paw expressed in percentage<sup>23</sup>.

#### *Histology and morphometry*

Four months after the injury, animals were deeply anesthetized and perfused with 4% paraformaldehyde in phosphate-buffered saline solution (0.1M, pH=7.4) and postfixed in 3% paraformaldehyde - 3% glutaraldehyde phosphate-buffered solution. The nerves were postfixed in osmium tetroxide (2%, 2 h, 4°C), dehydrated through ascending series of ethanol, and embedded in Epon resin. Semithin sections (0.5 µm) of the regenerated nerves were obtained by an ultramicrotome (Leica) stained with toluiden blue and examined by light microscopy. Representative images of the whole regenerated nerve were acquired at 10x magnification whereas higher magnification images at 100x were obtained to count the number of myelinated fibers with a digital camera (Olympus DP50) attached to a microscope (Olympus BX51). At least a 30% of the nerve area was acquired at the highest magnification in order to estimate the number of regenerated myelinated axons. Images were obtained at mid point of the tube and 3 mm distal. Measurements of both the nerve area and the number of stimulated myelinated fibers were carried out using ImageJ software (National Institute of Health)<sup>23</sup>. In cases where matrix remnants were present inside the regenerated nerve at the tube level, the area occupied by them was excluded for the measurements.

#### *Assessment of Schwann cell migration*

For the study of Schwann cell migration, 12 days after nerve section and tube repair leaving a 6 mm gap, animals were deeply anesthetized and perfused transcardiacally as above. The tubes were harvested and postfixed in 4% paraformaldehyde. 30 µm thick longitudinal sections of the regenerating cable were cut with a cryostat (Leica). Samples were incubated for 48 h with rabbit antibody against S100 (1:100, Immunostar) to label Schwann cells and

anti-NF-200 (1:1000, Millipore) to label regenerating axons. After washes, the sections were incubated for two hours with biotinylated IgG (1:200, Life Bioscience) and incubated overnight with secondary antibodies goat anti-rabbit conjugated with Alexa 488 and Alexa 594 (1:200, Life BioScience). To analyze Schwann cell migration, microphotographs of the regenerative front and Schwann cells were taken at 4× with a digital camera, acquired in Adobe Photoshop CS and photomerged. Using ImageJ software, resolution parameters were fixed and Schwann cells were followed from the proximal to the distal part of the implanted tube. The distance of the regenerated axonal front and the percentage of area occupied by migrating Schwann cells was calculated and compared.

#### *Statistical analysis*

Statistical comparison between groups and intervals in this study was analyzed by two-way ANOVA for repeated measurements followed by Bonferroni post-hoc tests. When analyzing histological results and the migration of Schwann cells in the short gap, results were analyzed by one-way ANOVA followed by Bonferroni post-test. Results were expressed as mean ± SEM and differences were considered significant when  $P < 0.05$ .

## **Results**

#### *Muscle reinnervation*

Initial evidence of reinnervation of the tibialis anterior and gastrocnemius muscles was found at 60 dpo in some animals of each group, with CMAPs of small amplitude. The CMAPs progressively increased in amplitude and were recorded in more animals over time, with a similar pattern for both muscles (Fig. 2A,B). At the end of the follow-up (120 dpo), reinnervation of the tibialis anterior and the gastrocnemius muscles was observed in 3 of 7 animals in the COL group, 2 of 7 in the LM group, 5 of 8 in the FN group, 4 of 7 in LM-St group, and 6 of 8 in the FN-St group. Significant differences ( $P < 0.05$ ) were observed at the final time point between the FN-St group and the COL and LM groups. Both FN and LM-St groups performed better than the LM group ( $P < 0.01$ ) (Fig. 2A,B).

At the more distal plantar interosseous muscles, onset of reinnervation was also found at 60 dpo. In this case, the CMAPs were of very small amplitude (less than 0.05 mV). At the end of the follow-up (120 dpo), evoked CMAPs of the plantar muscle were observed in 3 of 7 animals in the COL group (CMAP amplitude  $0.22 \pm 0.16$  mV), 2 of 7 in the LM group ( $0.08 \pm 0.08$  mV), 5 of 8 in the FN group ( $0.78 \pm 0.37$  mV), 4 of 7 in the LM-St group ( $0.44 \pm 0.28$

mV) and 5 of 8 in the FN-St group ( $0.67 \pm 0.37$  mV), but no significant differences were observed between groups (Fig. 2C).

The latencies of the registered CMAPs were shortened in time toward normal values. At the end of the follow-up, the latencies of the waves recorded on tibialis anterior and gastrocnemius muscles were significantly shorter in the FN, FN-St and LM-St groups than in the LM and COL groups (Fig. 2D,E).

The plantar CMAP latency averaged  $9.25 \pm 2.51$  ms in the COL group,  $8.37 \pm 2.52$  ms in the LM group,  $4.45 \pm 0.59$  ms in the FN group,  $5.83 \pm 0.60$  ms in the LM-St group and  $5.64 \pm 0.21$  ms in the FN-St group at the end of the follow-up, without significant differences between groups (Fig. 2F).

#### *Recovery of nociceptive sensibility*

Withdrawal responses to mechanical stimuli, evaluated with the Von Frey test, demonstrated absence of responses during the first 30 dpo, and therefore they were penalized with a cut off value of 40 g. From 60 to 120 dpo most of the rats showed withdrawal responses in the injured paw at lower stimulus intensity than in the contralateral side, indicating some degree of hyperalgesia. After elimination of the saphenous nerve at 120 dpo, withdrawal responses to mechanical stimuli in rats of the COL group ( $119.01 \pm 20.48$ g), the LM group ( $117.69 \pm 15.91$ g), and the FN group ( $112.53 \pm 8.87$ g), were slightly higher, but not significantly different ( $P > 0.05$ ) than in the contralateral side, whereas both LM-St ( $82.17 \pm 21.17$ g) and FN-St ( $81.96 \pm 13.84$ g) groups were slightly lower, but not significantly different compared to the contralateral paw (Fig. 2G), suggesting increased skin reinnervation in these two groups.

Withdrawal responses to thermal stimulation in the plantar test showed similar evolution than those observed for the Von Frey test. Animals had no response to heat stimuli on the denervated paw during the first 30 dpo. From 60 to 120 dpo, most rats showed withdrawal responses at lower stimulus intensity than in the contralateral side. When the saphenous nerve was cut, the withdrawal time of the injured paw at 122 dpo in rats of the COL group ( $126.37 \pm 22.72$ s), LM group ( $151.93 \pm 14.15$ s), FN group ( $118.97 \pm 30.97$ s), LM-St group ( $137.49 \pm 16.07$ s) and FN-St group ( $116.29 \pm 16.97$ s) were higher, although not significantly different to the contralateral intact side (Fig. 2H).

### *Histological results*

Macroscopic examination of the injured nerves after the 4 months follow-up showed that 3 of 7 animals in the COL group, 2 of 7 in the LM group, 5 of 8 in the FN group, 4 of 7 in the LM-St group and 6 of 8 in the FN-St group presented a regenerated cable inside the chitosan tube. Transverse sections of the regenerated nerves taken at the midpoint of the tube and at the distal segment were analyzed under light microscopy (Fig. 3). The mean number of myelinated fibers at the midpoint of the tube was higher in the FN group ( $5,673 \pm 2,501$ ) followed by FN-St ( $4,999 \pm 1,922$ ), LM-St ( $3,882 \pm 1,985$ ), COL ( $1,909 \pm 1,521$ ) and LM ( $614 \pm 838$ ) groups (Fig. 4A), without significant differences between groups due to high variability. The same pattern was observed in sections taken 3 mm distal to the end of the tube, where the number of myelinated fibers was higher in the FN group ( $3,098 \pm 1,813$ ) followed by FN-St ( $2,894 \pm 1,218$ ), LM-St ( $2,860 \pm 1,990$ ), COL ( $857 \pm 904$ ) and LM ( $568 \pm 774$ ) groups (Fig. 4B), without significant differences.

When analyzing the cross-sectional area of the regenerated nerve in the tube, the FN-St group had the largest area ( $0.26 \pm 0.09 \mu\text{m}^2$ ), followed by LM-St group ( $0.15 \pm 0.09 \mu\text{m}^2$ ), FN group ( $0.13 \pm 0.06 \mu\text{m}^2$ ), COL group ( $0.08 \pm 0.05 \mu\text{m}^2$ ) and LM group ( $0.03 \pm 0.02 \mu\text{m}^2$ ), with significant differences between the FN-St versus LM group ( $P < 0.05$ ). Distally, the same order was found for the size of the nerve, but without significant differences between groups (Figs. 4C,D).

When analyzing the residual matrices that were not degraded at the mid-level of the tube, the groups repaired with stabilized gels showed larger remnants (FN-St  $0.12 \pm 0.06 \mu\text{m}^2$ , and LM-St  $0.07 \pm 0.04 \mu\text{m}^2$ ), than groups with hydrated gels (FN  $0.02 \pm 0.02 \mu\text{m}^2$ , COL  $0.01 \pm 0.003 \mu\text{m}^2$  and LM  $0.005 \pm 0.003 \mu\text{m}^2$ ), but without significant differences between groups.

The percentage of regenerated animals with presence of distal axons and positive reinnervation of target muscles was also represented (Fig 4E).

### *Schwann cell migration*

Immunohistochemical labeling of the regenerating cable formed inside the tube at 12 dpo (Fig. 5A) revealed that the distance covered by the regenerating front, labeled against neurofilament heavy chain, was longest in the FN-St ( $5,214 \pm 124 \mu\text{m}$ ) and LM-St groups ( $4,778 \pm 198 \mu\text{m}$ ), followed by the FN ( $4,037 \pm 495 \mu\text{m}$ ) and LM ( $3,675 \pm 668 \mu\text{m}$ ) horizontally polymerized groups, and finally the COL group ( $1,906 \pm 954 \mu\text{m}$ ), with significant differences between the FN-St versus the COL group ( $P < 0.05$ ) (Fig. 5B).

Similarly, the area occupied by Schwann cells, labeled for S-100, was largest in the FN-St group ( $91.98 \pm 1.37$  %), followed by the FN ( $90.66 \pm 3.34$  %), LM-St ( $82.48 \pm 1.61$  %), LM ( $78.68 \pm 9.87$  %) and COL groups ( $67.03 \pm 9.23$  %), without significant differences between them (Fig. 5C).

## Discussion

In this study, we have compared the effect of the addition of laminin or fibronectin in a collagen type I based matrix, both incorporated either as fully-hydrated hydrogel fillers or stabilized and organized into longitudinally oriented scaffolds, within chitosan conduits to sustain axonal regeneration across a critical model of 15 mm gap resection of the sciatic nerve in rats. Our results show that addition of fibronectin in the collagen matrix enhanced nerve regeneration, and that stabilization and organization of the hydrogels into longitudinally oriented structures further increased the cases in which regeneration occurred over the 15 mm long gap. Furthermore, we investigated the effect of those matrices at short term, and found that the stabilization and organization of the initial matrix increased Schwann cell migration and axonal growth.

Here we have used a chitosan tube that was already proven to be more effective than the standard silicone tube for supporting axonal regeneration across limiting gaps in rats<sup>23</sup>. However, the percentage of success in this model is still far from the 100% success of an autograft, the gold standard repair technique to bridge long peripheral nerve gaps. Therefore, there is need to further improve the regenerative capability of these guides. Regeneration in tubular guides is dependent on the formation of an initial fibrin matrix which has to bridge the gap formed between the stumps. This fibrin cable provides a guidance surface to fibroblasts, blood vessels and Schwann cells to migrate from proximal and distal nerve stumps to populate the cable and sustain the advance of the regenerating axons<sup>6</sup>. Therefore, prefilling the tube with scaffolds can favor Schwann cell migration and facilitate regeneration across the conduits when the formation of the fibrin cable is limited.

In this work we have used a collagen type I hydrogel matrix as a base, that has previously been shown to allow axonal growth in 3D *in vitro* assays<sup>27</sup>. It is easy to manipulate and can be enriched with different extracellular matrix molecules, such as fibronectin or laminin, in a mixture that is permissive for regeneration both *in vitro* and *in vivo*<sup>28</sup>. Previous works have already shown that pre-filling a nerve conduit with ECM components supports axonal growth<sup>14,15,16,18</sup>, although the regeneration promoting capacity remains inferior compared to an autograft<sup>29</sup>. This limitation may be due to the composition, the density of the matrices and

the lack of alignment of their components<sup>18,30</sup> that may interfere with the migration of Schwann cells and the directed growth of axons along the conduit lumen. The longitudinal alignment of an ECM gel within a nerve conduit attempts to mimic the natural geometry of the endoneurial tubes in nerve grafts. Many efforts during the last years have focused on the development of novel tissue engineering techniques and biomaterials that can confer orientation upon cells and ECM, including the use of gradients, electrical and magnetic fields, and cellular self-alignment in response to tension in tethered collagen gels<sup>19,21,31</sup>. In addition to the regeneration support and guidance resulting from micro and nanoscale alignment of cells and collagen fibrils in the latter studies<sup>20,32</sup> rolling sheets of stabilized collagen hydrogel inside a conduit provides an additional level of meso-scale tissue structure than obtained from simply filling the conduit lumen with a fully hydrated hydrogel. Here we have isolated this variable, and directly compared the extent of nerve regeneration that results from using simple hydrogel fillers versus the same materials stabilized and rolled to provide some tissue architecture. The results indicate that the more organized matrix structure is beneficial in promoting regeneration even in the absence of self-aligned therapeutic cells and the accompanying nanofibrillar anisotropy of the collagen matrix.

Interestingly, we found that addition of fibronectin to the intratubular matrix increased the proportion of animals that regenerated, enhanced motor reinnervation and number of myelinated axons than the addition of laminin or the collagen matrix alone. Furthermore, when stabilized rolled gels were incorporated in the tube, the regeneration was further improved; in the FN-St group the proportion of animals that presented a regenerative cable after 4 months increased to 75% of the rats, whereas in the LM-St group it was 57% (Table 1). Both laminin and fibronectin have been used to promote nerve regeneration and provide support in long nerve gaps using various different approaches. A previous study compared the addition of laminin and/or fibronectin in tubular devices to repair long nerve gaps<sup>14</sup>. The authors filled silicone tubes with saline solution containing these ECM proteins, and found that the incidence of cable formation that bridged the gap was similar in all groups, although combination of both molecules increased the number of regenerating axons<sup>14</sup>. In contrast, we have found that the addition of fibronectin within a collagen-based matrix increased the percentage of regeneration across a critical gap compared to the laminin-containing matrix. These differences could be due to the composition and topographical conformation of the fibrils constituting the matrix used to fill the tube, which are important factors determining the rate of axonal regeneration<sup>18,30,33,34</sup>. The interaction between collagen type I and laminin or

fibronectin is not well characterized. It is possible that the addition of laminin to collagen matrices increase the thickness and density of the strands, whereas the combination of fibronectin and collagen might result in a better organization.

Microscopic examination of the regenerated nerves revealed presence of residual matrices at the tube level. Although larger remnants were found in the animals repaired with stabilized hydrogels, significant differences were not observed between groups. The appearance of these residual matrices may be attributed to the compact conformation of the stabilized gels, as previously reported<sup>31</sup>, in which enzymatic degradation by collagenase and other proteases was probably slower. However, as noted in the quantification of the number of myelinated fibers, such ECM remnants did not compromise axonal regeneration.

Since aligned type I collagen facilitates migration of Schwann cells *in vitro* compared to unaligned collagen gel<sup>21</sup>, and fibronectin plays an important role in migration of Schwann cells *in vitro* and into neural guides<sup>35</sup>, we wanted to evaluate migration of Schwann cells from the proximal and the distal stump. For that experiment we used a shorter gap, in order to guarantee the formation of the fibrin cable in all the animals. We observed that the regenerating axon front extended to longer distances in fibronectin and laminin stabilized rolled hydrogel groups compared to fully hydrated hydrogel matrices. Schwann cell migration was not significantly different between groups at 12 days using this gap length. However, the trend observed in the short gap between fibronectin and laminin groups may become a relevant difference in the long gap model and thus, the slight enhancement of Schwann cell migration into the tube may be decisive to sustain regeneration in a critical gap. Indeed, fibronectin aligned fibers were shown to provide an orientating cue for migrating fibroblasts and Schwann cells, and for neurite elongation<sup>36</sup>. Besides its effects on Schwann cell migration, the beneficial effects of fibronectin in nerve conduits can also be due to its supportive effect on viable Schwann cells<sup>35</sup>.

## **Conclusion**

The present study shows the importance of the conformation and organization of hydrogel matrix components on promoting regeneration after severe peripheral nerve injuries. Stabilization and rolling of collagen-based matrices, and enrichment with other ECM proteins improved the quality and quantity of the nerve repair process. The fibronectin-collagen stabilized rolled construct seems a promising candidate to be used as internal filler of tubular nerve conduits, allowing regeneration across a critical long gap in a significant number of

cases, by facilitating formation of the fibrin cable, Schwann cell migration and growth of regenerating axons through the neural conduit.

## REFERENCES

1. Deumens R, Bozkurt A, Meek MF, et al. Repairing injured peripheral nerves: Bridging the gap. *Prog Neurobiol* 2010;92:245–276.
2. Doolabh V, Hertl M, Mackinnon S. The role of conduits in nerve repair: a review. *Rev Neurosci* 1996;7:47–84.
3. Gu X, Ding F, Yang Y, Liu J. Construction of tissue engineered nerve grafts and their application in peripheral nerve regeneration. *Prog Neurobiol*.2011;93:204–230.
4. Yannas IV, Hill BJ. Selection of biomaterials for peripheral nerve regeneration using data from the nerve chamber model. *Biomaterials* 2004;25:1593-1600.
5. Lundborg G, Dahlin L, Danielsen N, et al. Nerve regeneration in silicone chambers: influence of gap length and of distal stump components. *Exp Neurol* 1982;76:361-375.
6. Williams L, Longo F, Powell H, Lundborg G, Varon S. Spatial-temporal progress of peripheral nerve regeneration within a silicone chamber: parameters for a bioassay. *J Comp Neurol* 1983;218:460–470.
7. Madison R, da Silva C, Dikkes, P, Sidman R, Chiu T. Peripheral nerve regeneration with entubulation repair: comparison of biodegradable nerve guides versus polyethylene tubes and the effects of a laminin-containing gel. *Exp Neurol* 1987;95:378–390.
8. Butí M, Verdú E, Labrador RO, Vílches J, Forés J, Navarro X. Influence of physical parameters of nerve chambers on peripheral nerve regeneration and reinnervation. *Exp Neurol* 1996;137:26-33.
9. Gómez N, Cuadras J, Butí M, Navarro X. Histological assesment of sciatic nerve regeneration following resection and graft or tube repair in the mouse. *Restor Neurol Neurosci* 1996;10:187-196.
10. Rutka J, Apodaca G, Stern R, Roseblum M. The extracellular matrix of the central and peripheral nervous systems: structure and function. *J Neurosurg* 1988;69:155–170.
11. Gonzalez-Perez F, Udina E, Navarro X. Extracellular matrix components in peripheral nerve regeneration. *Int Rev Neurobiol* 2013;108:257–275.
12. Baron-Van Evercooren A, Kleinman HK, Ohno S, Marangos P, Schwartz JP, Dubois-Dalcq M. Nerve growth factor, laminin, and fibronectin promote neurite growth in human fetal sensory ganglia cultures. *J Neuroscience Res* 1982;8:179–93.
13. Gardiner NJ, Moffatt S, Fernyhough P, Humphries M. J, Streuli CH, Tomlinson, DR. Preconditioning injury-induced neurite outgrowth of adult rat sensory neurons on

- fibronectin is mediated by mobilisation of axonal alpha5 integrin. *Mol Cell Neurosci* 2007;35:249–260.
14. Bailey S, Eichler M, Villadiego A, Rich KM. The influence of fibronectin and laminin during Schwann cell migration and peripheral nerve regeneration through silicon chambers. *J Neurocytol* 1993;22:176–184.
  15. Chen YS, Hsieh CL, Tsai CC, et al. Peripheral nerve regeneration using silicone rubber chambers filled with collagen, laminin and fibronectin. *Biomaterials* 2000;21:1541–1547.
  16. Labrador R, Butí M, Navarro X. Influence of collagen and laminin gels concentration on nerve regeneration after resection and tube repair. *Exp Neurol* 1998;149:243–252.
  17. Liu WQ, Martinez JA, Durand J, Wildering W, Zochodne DW. RGD-mediated adhesive interactions are important for peripheral axon outgrowth in vivo. *Neurobiol Dis* 2009;34:11–22.
  18. Madison RD, Da Silva CF, Dikkes P. Entubulation repair with protein additives increases the maximum nerve gap distance successfully bridged with tubular prostheses. *Brain Res* 1988;447:325–334.
  19. Verdú E, Labrador RO, Rodríguez FJ, Ceballos D, Forés J, Navarro X. Alignment of collagen and laminin-containing gels improve nerve regeneration within silicone tubes. *Restor Neurol Neurosci* 2002;20:169–179.
  20. Georgiou M, Bunting SC, Davies HA, Loughlin AJ, Golding JP, Phillips JB. Engineered neural tissue for peripheral nerve repair. *Biomaterials* 2013;34:7335–7343.
  21. Dubey N, Letourneau PC, Tranquillo RT. Guided neurite elongation and schwann cell invasion into magnetically aligned collagen in simulated peripheral nerve regeneration. *Exp Neurol* 1999;158:338–350.
  22. Bellamkonda RV. Peripheral nerve regeneration: an opinion on channels, scaffolds and anisotropy. *Biomaterials* 2006;27:3515–3518.
  23. Gonzalez-Perez F, Cobianchi S, Geuna S, et al. Tubulization with chitosan guides for the repair of long gap peripheral nerve injury in the rat. *Microsurgery* 2015;35:300–308.
  24. Phillips JB, Brown R. Micro-structured materials and mechanical cues in 3D collagen gels. *Methods Mol Biol* 2011;695:183–196.

25. Navarro X, Butí M, Verdú E. Autotomy prevention by amitriptyline after peripheral nerve section in different strains of mice. *Restor Neurol Neurosci* 1994;6:151–157.
26. Cobianchi S, de Cruz J, & Navarro X. Assessment of sensory thresholds and nociceptive fiber growth after sciatic nerve injury reveal the differential contribution of collateral reinnervation and nerve regeneration to neuropathic pain. *Exp Neurol* 2014;255:1–11.
27. Allodi I, Guzmán-Lenis MS, Hernández J, Navarro X, Udina E. In vitro comparison of motor and sensory neuron outgrowth in a 3D collagen matrix. *J Neurosci Methods* 2011;198:53–61.
28. Gonzalez-Perez F, Alé A, Santos D, et al. Substratum preferences of motor and sensory neurons in postnatal and adult rats. *Eur J Neurosci* 2016;43:431–442.
29. Rodríguez FJ, Verdú E, Ceballos D, Navarro X. Nerve guides seeded with autologous schwann cells improve nerve regeneration. *Exp Neurol* 2000;161:571–584.
30. Labrador R, Butí M, Navarro X. Peripheral nerve repair: role of agarose matrix density on functional recovery. *Neuroreport* 1995;6:2022–2036.
31. Ceballos D, Navarro X, Dubey N, Wendelschafer-Crabb G, Kennedy WR, Tranquillo RT. Magnetically aligned collagen gel filling a collagen nerve guide improves peripheral nerve regeneration. *Exp Neurol* 1999;158:290–300.
32. Georgiou M, Golding JP, Loughlin AJ, Kingham PJ, Phillips JB. Engineered neural tissue with aligned, differentiated adipose-derived stem cells promotes peripheral nerve regeneration across a critical sized defect in rat sciatic nerve. *Biomaterials* 2015;37:242–251.
33. Balgude AP, Yu X, Szymanski A, Bellamkonda RV. Agarose gel stiffness determines rate of DRG neurite extension in 3D cultures. *Biomaterials* 2001;22:1077–1084.
34. Willits R, Skornia S. Effect of collagen gel stiffness on neurite extension. *J Biomater Sci Polym Ed* 2004;15:1521–1531.
35. Mosahebi A, Wiberg M, Terenghi G. Addition of fibronectin to alginate matrix improves peripheral nerve regeneration in tissue-engineered conduits. *Tissue Eng* 2003;9:209–218.
36. Ahmed Z, Brown RA. Adhesion, alignment, and migration of cultured Schwann cells on ultrathin fibronectin fibres. *Cell Motil Cytoskeleton* 1999;42:331–343.

## Figure Legends

Figure 1. Representative images of the stabilization and rolling technique. ABS moulds were filled with a collagen solution and let to gelify and stabilize for 24h in the incubator at 37°C (A). The excess of liquid was removed using absorbant pads for 15 minutes (B). The gel was carefully removed from the mould and inserted in a longitudinally cut chitosan guide (C) and sealed prior to implantation (D).

Figure 2. Mean amplitude of the compound muscle action potential (CMAP) of tibialis anterior (A), gastrocnemius (B) and plantar muscles (C) of the injured hindlimb of the rats during 4 months after sciatic nerve lesion and repair. \* $P < 0.05$  fibronectin vs laminin enriched groups; <sup>†</sup> $P < 0.05$  fibronectin vs collagen group. Mean latencies of the tibialis anterior (D), gastrocnemius (E) and plantar (F) CMAPs recorded in the regenerated rats during the 4 months follow-up. \* $P < 0.05$ . Mechanical (G) and thermal (H) algometry test results. Values are expressed as percentage of withdrawal threshold to mechanical and thermal stimuli applied to the lateral side of the injured paw versus the contralateral uninjured paw. Horizontal dotted lines represent the normalized baseline values. Vertical dotted lines indicate when the saphenous nerve was cut.

Figure 3. Micrographs of semithin sections of the regenerated nerve taken at the midpoint of the tube 4 months after sciatic nerve resection and repair from a representative animal of collagen group, laminin group, fibronectin group, laminin stabilized group and fibronectin stabilized group. The whole regenerated nerve is shown in the left panels; scale bar = 500  $\mu\text{m}$ .

Figure 4: Estimated number of regenerated myelinated fibers in the regenerated nerve at the mid-tube (A) and 3 mm distal (B) to the tube 4 months after sciatic nerve resection and repair. Cross-sectional area of the nerve at mid-tube (C) and 3 mm distal (D) levels. Animals with no regenerated nerve were also included (with null values) in the calculation. \*  $P < 0.05$ . Plot representing the percentage of regenerated nerves found at 120 dpo (E).

Figure 5. Representative images of longitudinal sections of sciatic nerves from rats injured and repaired with a chitosan conduit leaving a 6 mm gap in the collagen, laminin, fibronectin, laminin stabilized and fibronectin stabilized groups. 12 days after the surgery, regenerated axons were labeled with NF-200 (left panels), Schwann cells were labeled with S-100 (central panels), and the images were photomerged (right panels) with DAPI (blue). Scale bar = 1 mm

(A). Length of the front of axonal growth from the proximal end of the tube (B) and percentage of the nerve cable area occupied by migrating Schwann cells (C). \*  $P < 0.05$ .

Table 1. Comparison of results of muscle reinnervation and nerve regeneration from this study in which a 15 mm gap of the sciatic nerve was repaired with a chitosan conduit prefilled with ECM matrices with results obtained after repair with a hollow chitosan conduit and an autograft in a previous study<sup>23</sup>.

Fig 1:

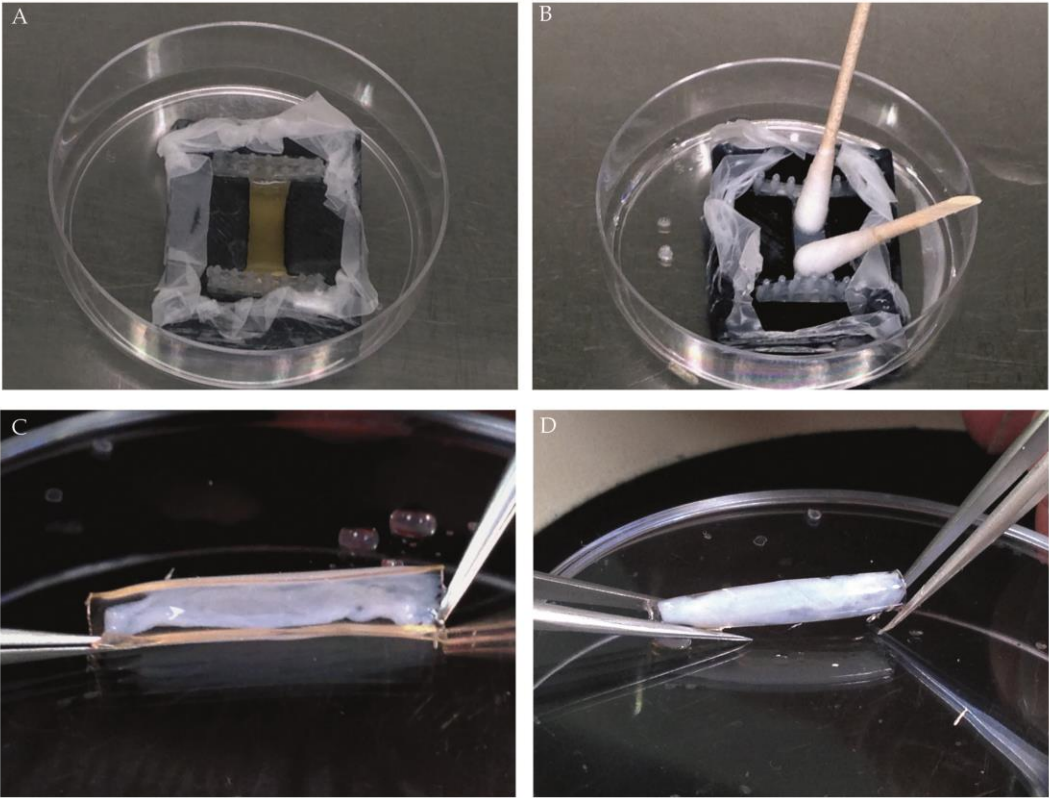


Fig 2:

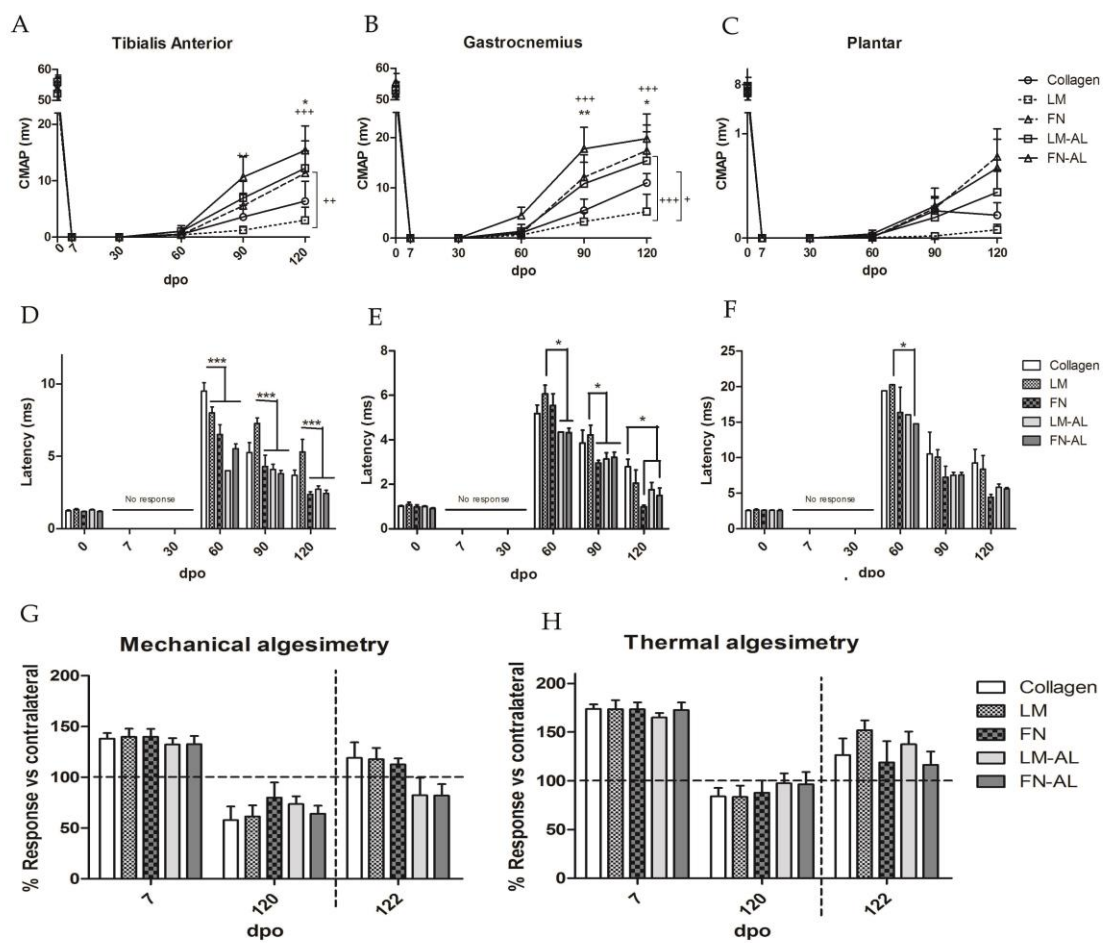


Fig 3:

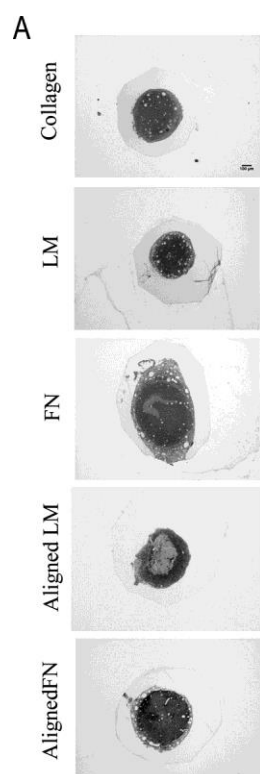


Fig 4:

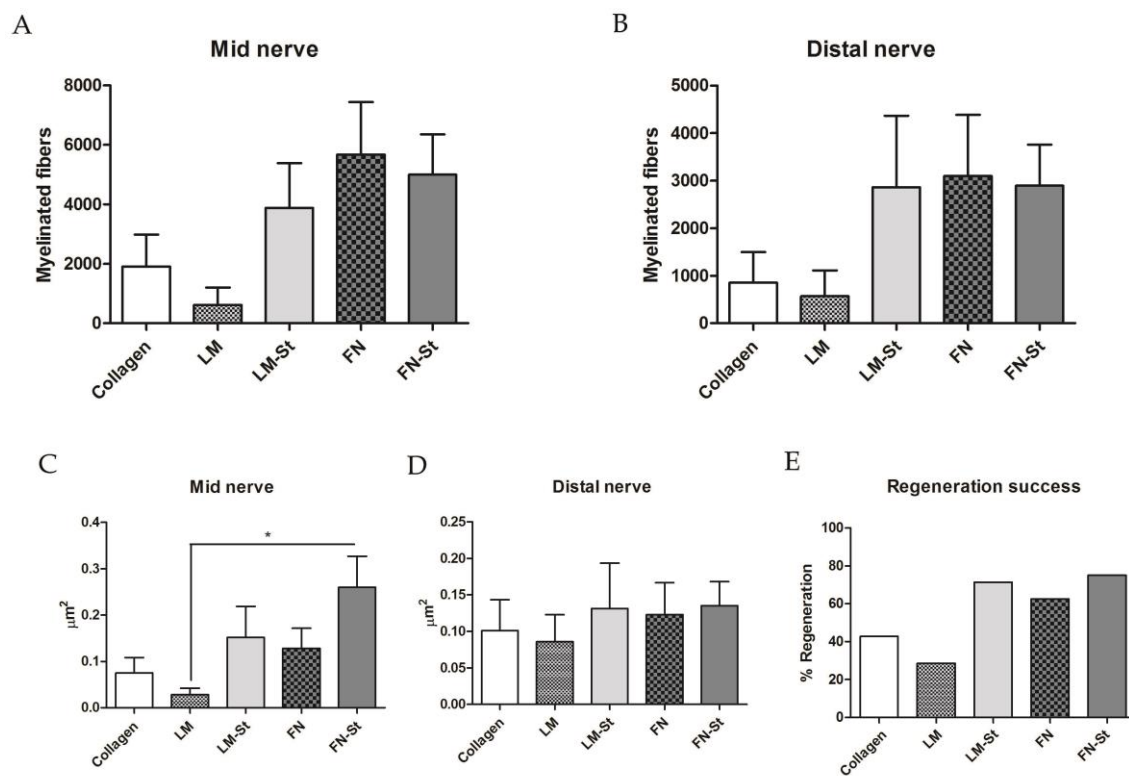


Fig 5:

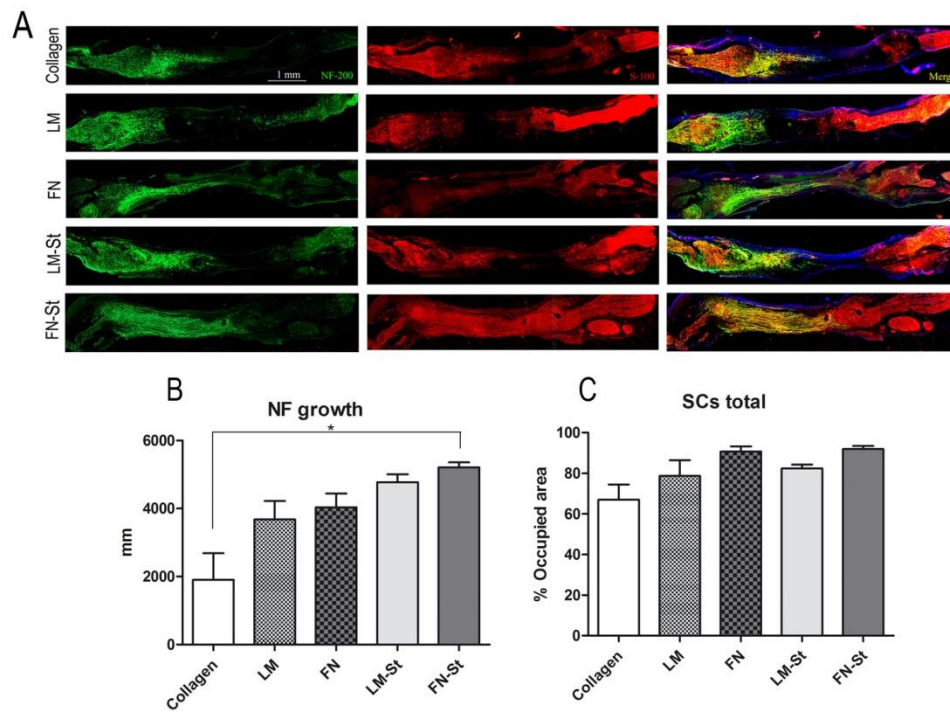


Table 1:

	% Recovery TA m	% Recovery PI m	Regenerated cable	Muscle reinnervation
<b>AG</b>	60%	33%	7/7	7/7
<b>Hollow Ch</b>	18%	8%	5/10	4/10
<b>COL</b>	12%	3%	3/7	3/7
<b>LM</b>	12%	1%	2/7	2/7
<b>FN</b>	21%	10%	5/7	5/7
<b>LM-St</b>	22%	6%	4/7	4/7
<b>FN-St</b>	29%	10%	6/8	6/8